HHS Public Access

Author manuscript

Oral Dis. Author manuscript; available in PMC 2024 July 08.

Published in final edited form as:

Oral Dis. 2024 April ; 30(3): 1350–1359. doi:10.1111/odi.14551.

CACNA1S mutation-associated dental anomalies: A calcium channelopathy

P. Kantaputra[1,2], **A. Butali**[3,4], **S. Eliason**[5], **C. Chalkley**[5], **S. Nakornchai**[6], **C. Bongkochwilawan**[1,2], **K. Kawasaki**[7], **A. Kumchiang**[8], **C. Ngamphiw**[9], **S. Tongsima**[9], **J. R. Ketudat Cairns**[10,11], **B. Olsen**[12], **W. Intachai**[1,2], **A. Ohazama**[7], **A. S. Tucker**[13], **B. A. Amendt**[3,5]

[1]Center of Excellence in Medical Genetics Research, Faculty of Dentistry, Chiang Mai University, Chiang Mai, Thailand

[2]Division of Pediatric Dentistry, Department of Orthodontics and Pediatric Dentistry, Faculty of Dentistry, Chiang Mai University, Chiang Mai, Thailand

[3]Iowa Institute of Oral Health Research, University of Iowa, Iowa City, Iowa, USA

[4]Department of Oral Pathology, Radiology and Medicine, College of Dentistry, University of Iowa, Iowa City, Iowa, USA

[5]Department of Anatomy and Cell Biology, Craniofacial Anomalies Research Center, University of Iowa, Iowa City, Iowa, USA

[6]Department of Pediatric Dentistry, Faculty of Dentistry, Mahidol University, Bangkok, Thailand

Correspondence: P. Kantaputra, Division of Pediatric Dentistry, Department of Orthodontics and Pediatric Dentistry, Faculty of Dentistry, Chiang Mai University, Chiang Mai 50200, Thailand. dentaland17@gmail.com, A. S. Tucker, Centre for Craniofacial and Regenerative Biology, King's College London, Floor 27 Guy's Hospital, London Bridge, London SE1 9RT, UK. abigail.tucker@kcl.ac.uk.

AUTHOR CONTRIBUTIONS

P. Kantaputra: Conceptualization; investigation; funding acquisition; writing – original draft; methodology; validation; visualization; writing – review and editing; formal analysis; project administration; supervision; resources; data curation. **A. Butali:** Conceptualization; investigation; methodology; validation; writing – original draft; writing – review and editing; visualization; formal analysis. **S. Eliason:** Conceptualization; investigation; writing – original draft; methodology; validation; visualization; writing – review and editing; formal analysis; data curation. **C. Chalkley:** Conceptualization; investigation; writing – original draft; methodology; validation; visualization; writing – review and editing; formal analysis. **S. Nakornchai:** Conceptualization; investigation; writing – original draft; methodology; validation; visualization; writing – review and editing. **C. Bongkochwilawan:** Conceptualization; investigation; writing – original draft; methodology; validation; visualization; writing – review and editing. **K. Kawasaki:** Conceptualization; investigation; writing – original draft; methodology; validation; visualization; writing – review and editing. **A. Kumchiang:** Conceptualization; investigation; writing – original draft; methodology; validation; visualization; writing – review and editing. **C. Ngamphiw:** Conceptualization; investigation; writing – original draft; methodology; validation; visualization; writing – review and editing; data curation; software. **S. Tongsima:** Conceptualization; investigation; writing – original draft; methodology; validation; visualization; writing – review and editing; software; formal analysis; data curation. **J. R. Ketudat Cairns:** Conceptualization; investigation; writing – original draft; methodology; validation; visualization; writing – review and editing; software; data curation. **B. Olsen:** Conceptualization; investigation; writing – original draft; methodology; validation; visualization; writing – review and editing. **W. Intachai:** Conceptualization; investigation; writing – original draft; methodology; validation; visualization; writing – review and editing; formal analysis; data curation. **A. Ohazama:** Conceptualization; investigation; writing – original draft; methodology; validation; visualization; writing – review and editing; formal analysis. **A. S. Tucker:** Conceptualization; investigation; writing – original draft; methodology; validation; visualization; writing – review and editing; formal analysis. **B. A. Amendt:** Conceptualization; investigation; writing – original draft; methodology; validation; visualization; writing – review and editing.

CONFLICT OF INTEREST STATEMENT

The authors declare that there are no conflicts of interest.

SUPPORTING INFORMATION

Additional supporting information can be found online in the Supporting Information section at the end of this article.

[7]Division of Oral Anatomy, Department of Oral Biological Science, Niigata University Graduate School of Medical and Dental Sciences, Niigata, Japan

[8]Na-Chauk Hospital, Na-Chauk, Maha Sarakham, Thailand

[9]National Biobank of Thailand, National Science and Technology Development Agency (NSTDA), Thailand Science Park, Khlong Luang, Pathum Thani, Thailand

[10]Center for Biomolecular Structure, Function and Application, School of Chemistry, Institute of Science, Suranaree University of Technology, Nakhon Ratchasima, Thailand

[11]Laboratory of Biochemistry, Chulabhorn Research Institute, Bangkok, Thailand

[12]Department of Developmental Biology, Harvard School of Dental Medicine, Boston, Massachusetts, USA

[13]Centre for Craniofacial and Regenerative Biology, King's College London, London, UK

Abstract

Objectives: To identify the molecular etiology of distinct dental anomalies found in eight Thai patients and explore the mutational effects on cellular functions.

Materials and Methods: Clinical and radiographic examinations were performed for eight patients. Whole exome sequencing, mutant protein modelling, qPCR, western blot analysis, scratch assays, immunofluorescence, confocal analysis, in situ hybridization, and scanning electron micrography of teeth were done.

Results: All patients had molars with multiple supernumerary cusps, single-cusped premolars, and a reduction in root number. Mutation analysis highlighted a heterozygous c.865A>G; p.Ile289Val mutation in *CACNA1S* in the patients. CACNA1S is a component of the slowly inactivating L-type voltage-dependent calcium channel. Mutant protein modeling suggested that the mutation might allow leakage of Ca^{2+} or other cations, or a tightening, to restrict calcium flow. Immunohistochemistry analysis showed expression of Cacna1s in the developing murine tooth epithelium during stages of crown and root morphogenesis. In cell culture, the mutation resulted in abnormal cell migration of transfected CHO cells compared to wildtype *CACNA1S*, with changes to the cytoskeleton and markers of focal adhesion.

Conclusions: The malformations observed in our patients suggest a role for calcium signaling in organization of both cusps and roots, affecting cell dynamics within the dental epithelium.

Keywords

calcium homeostasis; hypodontia; root malformation; single-rooted molar; supernumerary cusps; tooth development

1 | INTRODUCTION

An important part of tooth development is the folding of the dental epithelium to generate cusps, with more folding generating more cusps. This occurs at the cap and bell stages and is regulated by the primary and secondary enamel knots, transient structures of non-proliferative cells, located in the inner dental epithelium. The number, shape, size, and

location of cusps determine the morphology of the occlusal surface of a molar (Jernvall & Thesleff, 2012). Generally, mutations in tooth-related genes result in teeth with less complexity. In mice, loss of sonic hedgehog (Shh) signaling inhibits cusp formation and patterning and results in fusion of adjacent teeth (Ahn et al., 2010; Cho et al., 2011; Harjunmaa et al., 2012). In contrast, tooth crown complexity can be increased substantially after overexpression of pathways. Increased ectodysplasin A (EDA) signaling alone led to an increase in cusp number (Kangas et al., 2004; Tucker et al., 2004), while the number of cusps was doubled when SHH, EDA, and activin A signaling pathways were experimentally manipulated together. An increase in dental complexity may therefore require multiple changes in developmental regulation (Harjunmaa et al., 2012). In keeping with this, increased number of cusps in humans is rarer than a loss of cusps.

Genetic analysis of five Thai families with additional molar cusps recently identified the changes in tooth morphogenesis to be caused by a heterozygous missense mutation (c.865A>G; p.Ile289Val) in *calcium channel voltage-dependent, L-type, alpha-1S subunit* (*CACNA1S*; MIM 114208) (Laugel-Haushalter et al., 2018), highlighting a link between calcium channels and tooth morphogenesis. *CACNA1S* encodes $Ca_v1.1$, one of the subunits ($Ca_v1.1$, 1.2, 1.3, 1.4) of the slowly inactivating L-type voltage-dependent calcium channel, known as the dihydropyridine (DHP) channel. The alpha 1 subunit contains four homologous repeats, each containing six transmembrane segments (S1–S6) organized in clockwise manner into a canonical voltage-gated ion channel fold (Schartner et al., 2017; Wu et al., 2016). *CACNA1S* encodes the pore-forming subunit of the DHP channel. The missense mutation in the Thai patients is in the first pore-forming intramembrane domain between S5 and S6, close to the three amino acid residues involved in calcium selectivity (Laugel-Haushalter et al., 2018). In muscles, the DHP channel regulates Ca^{2+} release from the sarcoplasmic reticulum with the channel acting as a sensor of depolarization, allowing calcium release and diffusion (Schartner et al., 2017). As such, it has a vital role in excitation-contraction coupling to generate muscle contraction. Mice and *Drosophila* with defective *Cacna1s* are embryonically lethal, with a complete absence of skeletal muscle contraction (Eberl et al., 1998; Knudson et al., 1989), while the downregulation of *Cacna1s* in adult mice led to muscle atrophy (Piétri-Rouxel et al., 2010). Mutations in the *CACNA1S* gene have been reported in patients with a number of disorders including hypokalemic periodic paralysis, thyrotoxic periodic paralysis, and malignant hyperthermia (Schartner et al., 2017). In addition to a role in tooth morphogenesis, *CACNA1S* has been previously linked with both timing of tooth eruption and tooth agenesis in genome wide screens (Geller et al., 2011; Jonsson et al., 2018), while other calcium channels have also been associated with differentiation of dental hard tissues (Duan, 2014).

Here, we report eight Thai patients from three unrelated families affected with very unusual dental malformations consisting of multiple supernumerary molar cusps, molars with single roots, and single prominent cusped premolars. Confirming the link between calcium channels and tooth morphogenesis, we identified the same causative mutation in *CACNA1S*. By investigating the effects of this *CACNA1S* mutation on patient hard tooth tissue and using murine models and cell lines to analyze the effects of the mutation on cellular functions, our data provide a novel understanding of how mutation in this key calcium channel subunit may impact odontogenesis.

2 | MATERIALS AND METHODS

2.1 | Ethics statement

The study was conducted in accordance with the Declaration of Helsinki and national guidelines. Informed consent was obtained from the patients and/or their parents in accordance with the regulations of the Human Experimentation Committee of the Faculty of Dentistry, Chiang Mai University.

2.2 | Scanning electron micrography

The tooth that was studied under SEM was an exfoliated primary molar. The tooth was split using a dental chisel and hammer, rinsed with water, and hot air dried.

2.3 | Whole exome sequencing

Genomic DNA was extracted from the saliva according to the protocol from the Oragene® collecting kit (DNA Genotek Inc.). Five DNA samples of three affected (II-3, III-1, and III-3) and two unaffected members (I-1 and II-1) of Family 1 were sequenced by a whole exome sequencing (WES) protocol to detect variants within protein-coding genes (Figure 1a).

Exon capture was performed using the SureSelect target Enrichment system (Marcogen Inc.). Pair-end sequencing was then performed on a HiSeq 2000/2500 sequencing machine. A Burrows-Wheeler Alignment tool (BWA-0.7.17) was used to align the 100-bp reads from the sequencer to the human reference genome (hg19 from UCSC, GRCh37 from NCBI). Single-nucleotide variants (SNVs) and small INDEL variants were identified by Picard (picard-tool-2.9.0), Genome analysis toolkit (GATKv3.8.1), and Ensembl Variant Effect Predictor tool (version 95). Mutation discovery was based on variants called from WES of eight family members (three affected and two unaffected members) (Figure 1a).

The details of the variant prioritization process are shown in Figure 2. The 1,284,956 variants used in this process were identified by Genomics analysis toolkit (GATK) best practices (McKenna et al., 2010). These variants were assigned with varying quality scores, based on GATK Variant Quality Score Recalibration. The output “CombineGVCF” file included variants from three affected probands and two unaffected parents. These variants were processed using GENMOD (Magnusson, 2018) to provide variants with mode-of-inheritance scenarios for the proband, leaving 1,113,248 variants that fit with GENMOD segregation models. Note that we only considered variants with high confidence, which are defined by having genotype quality >20 and total depth >10 across all affected samples. Thus, this process filtered out a large number of variants leaving the remaining 4090 variants to be annotated using Ensembl Variant Effect Predictor (VEP) build 105 with dbNSFP plugin version 4.3a. We considered very rare variants based on public aggregated allele frequencies (<0.0001) from 1000G, gnomAD exomes and gnomAD genomes allele and the Thai exome database (T-Rex dB) with aggregated allele frequencies <0.01. The very rare 71 variants were further filtered out, leaving 57 variants by keeping only those predicted to have high and moderate impact, which included splice accepter, frameshift, stop gained and missense consequences. Next, we considered the 32 autosomal dominant variants with allele

balance of heterozygous or variant allele frequency >0.2, leaving 26 variant candidates. Finally, we considered only the canonical isoform of these variants that have the predicted functions as "(D)eleterious or (D)amaging" by MetaSVM (Dong et al., 2015), MetaLR (Dong et al., 2015) and MetaRNN (Li et al., 2022). Only 1 variant remained, and it was further validated by Sanger sequencing to support the etiologic hypothesis (Figure 2).

2.4 | Mutation analysis

In order to validate the mutation identified by WES, bidirectional direct sequencing (Functional Biosciences) and Sequencher 4.8 Sequence analysis software (Genecodes) were used to analyze the presence of variants in all affected and unaffected family members. Co-segregation between genotype and phenotype within the family was analyzed.

2.5 | Mutant protein modelling

The structure of $Ca_v1.1$ was modeled with the Swiss Model Protein Modeling server (Waterhouse et al., 2018) based on the structure of the rabbit $Ca_v1.1$ protein (Wu et al., 2016), which shares a 96% amino acid sequence identity with the human protein and is identical in the region of the 1289 residue.

2.6 | Immunohistochemistry

CD-1 strain mice were used in this study. To accurately assess the age of embryos, somite pairs were counted, and the stage confirmed using morphological criteria, for example, relative sizes of maxillary and mandibular primordia, extent of nasal placode invagination, and the size of limb buds. Embryo heads were fixed in 4% buffered paraformaldehyde, wax embedded, and serially sectioned at 7 μm. Sections were incubated with an antibody against CACNA1S (ThermoFisher; MA3–920). The tyramide signal amplification system was used (Parkin Elmer Life Science) to detect the CACNA1S antibody.

2.7 | Cell lines, qPCR, and western blot analysis

CHO lines were made by stable integration of pCDNA3.1, *CACNA1S* Wt and *CACNA1S* mutant constructs (linearized to increase integration) followed by selection with G418 at 400 μg/ml. These cells were used to isolate total RNA was isolated using Triazol (Sigma). RNA was precipitated, ribosomal bands assessed using gel electrophoresis and the RNA quantitated using a nanodrop. qPCR and Western blot analysis were performed as previously described (Gao et al., 2015) with antibodies against GAPDH (Santa Cruz) as a control protein, and against the FLAG-tag (Abcam) on the recombinant CACNA1S.

2.8 | Scratch assays

Scratch assays were performed on CHO cells and CHO lines pCDNA3.1, *CACNA1S* WT, or *CACNA1S* mutant DNA, as previously described (Liu et al., 2017). Photos were taken at the time of the scratch, 1 and 24 h post scratch. Each condition had four independent wells and each well had four scratches. The distance of the scratch was quantitated with imageJ and expressed as the rate of scratch migration, in μm/h.

2.9 | IF and confocal analysis

Untransfected CHO cells or stable lines with pCDNA3.1, *CACNA1S* WT, or *CACNA1S* mutant DNA were fixed and permeabilized as previously described (Li et al., 2014). FLAG AB (Cell Signaling, Inc), Phalloidin-TRITC (Sigma Aldrich), Donkey anti-mouse A488 (Jackson immunoreagents) and 4',6-diamidino-2-phenylindole (DAPI) were used for this analysis on a Zeiss 680 confocal microscope. The amount of CACNA1S (green) and phalloidin (red) was quantitated using ImageJ and compared with the amount of DAPI (blue) for multiple staining's ($n = 5$ for each).

3 | RESULTS

3.1 | Whole exome sequencing confirmed a mutation in *CACNA1S* cause supernumerary molar cusps

Eight Thai patients from three unrelated families were analyzed as part of the study (Figure 1a–k). WES was performed in three affected (II-3, III-1, and III-3) and two unaffected patients (I-1 and II-1) of family 1. Each patient had similar dental anomalies consisting of multiple gigantic cusps resembling the morphology of dens evaginatus, and premolars with single prominent cusps (Figure 1d,e,g,h–j; Figure S1) and single-rooted molars (Figure 1f,k). Both primary and permanent dentitions were affected (Figure 1d–k; Figures S1 and S2).

Whole exome sequencing and validation by Sanger sequencing confirmed the heterozygous c.865A>G; p.Ile289Val mutation (NM_000069.2; NP_000060.2; rs139920212) in the DNA of six affected, but not two unaffected family members of Family 1. This heterozygous base substitution co-segregates with the dental phenotype in this family (Figure S3). Furthermore, this variant was not found in our in-house exome database constructed from 925 exome patient data. Sanger sequencing identified the same mutation in the patients 7 and 8 of families 2 and 3, respectively. All unaffected family members did not carry the mutation (Figure S3). This verifies the dental phenotype generated by the heterozygous base substitution c.865A>G in *CACNA1S*, confirming the role of this calcium channel in tooth morphogenesis.

3.2 | Structure of the dental hard tissues appeared unaffected by the mutation

Calcium channels have previously been linked to a role in odontoblast differentiation and enamel maturation (Duan, 2014), with antibodies against 1.4 DHP highlighting the presence of L-type calcium channels accumulating on the apical pole of polarised odontoblasts during dentinogenesis (Seux et al., 1994). Mutations in *CACNA1C* lead to Timothy syndrome (OMIM 601005), an autosomal dominant disorder characterized dentally by small, misplaced teeth with enamel hypoplasia (Splawski et al., 2004). We therefore investigated the structure of the enamel, dentin and cementum of a naturally exfoliated tooth from a patient with a *CACNA1S* mutation using SEM. Normal ultrastructure of the enamel, dentin and cementum were observed, suggesting that the *CACNA1S* subunit does not play a role in these later stages of hard tissue formation (Figure 3a,b).

3.3 | CACNA1S is expressed in the murine dental epithelium during early tooth development

Cacna1s has previously been shown to be expressed in mouse incisors and molars at embryonic day (E)14.5 using a transcriptomic dataset (Laugel-Haushalter et al., 2018). In order to understand the spatial expression of Cacna1s in the tooth we, therefore, turned to immunohistochemistry. No significant expression in the developing tooth could be detected at E11.5 (Figure 4a). Cacna1s was expressed in the developing dental epithelium at E12.5 and E13.5, with high levels in the forming musculature of the lower jaw and tongue (Figure 4b–d). At E14.5, Cacna1s expression was observed in the dental epithelium, but interestingly expression was excluded from the enamel knot (Figure 4e). Cacna1s was expressed in both upper and lower molar tooth epithelium at these stages. In addition, Cacna1s expression was observed in Hertwig's epithelial root sheath (HERS) the epithelial cells responsible for guiding root development (Figure 4f). This dynamic expression pattern suggests a role in both tooth crown and root morphogenesis.

3.4 | Mutant protein impacts the functions of the calcium channel

To understand how this mutation impacted the structure of the protein, a model was constructed to assess the position of the mutation within the α1 subunit. The structure of the rabbit $Ca_v1.1$ complex was previously determined (Wu et al., 2016) and the human α1 subunit has recently been modelled (Martinez-Ortiz & Cardozo, 2018). The modelling highlighted that the loss of a methyl group in the conversion of Ile to Val would cause a small change in the hydrophobic packing next to the selectivity filter. Although this might be expected to make more space and result in a loosening of the filter to allow leakage of Ca^{2+} or other cations, the repacking could also result in a tightening to restrict calcium flow (Figure 3c,d).

To test the effect of the mutation, we investigated the effects of overexpression of the wildtype (WT) and mutant proteins on cell behavior. For this, we chose CHO cells, as they do not express *CACNA1S*. Stable lines expressing control DNA, *CACNA1S* WT and *CACNA1S* mutant constructs were generated, with overexpression confirmed by qPCR (Figure 5a). Western blotting was performed to determine the presence and stability of protein in the WT and mutant overexpression lines and we were able to confirm that a protein of >100 kDa was detected using FLAG antibodies in both WT and mutant lines, consistent with the size of *CACNA1S* (Figure 5b). These results confirm that the constructs produce RNA and protein, and that the wildtype and mutant proteins are both stable in CHO cells.

Having established the lines, we then tested the impact of the mutation. Calcium influx has been linked to changes in the cytoskeleton, thereby impacting migration (Tsai et al., 2015). We therefore used a scratch assay to compare the speed of migration in the three lines over a 24-h period (Figure 5c,d). The CHO cells migrated slowly, with a clear gap evident after 24 h. In contrast, the cells over-expressing wildtype *CACNA1S*, displayed an accelerated closure of the gap, and returned to confluency at 24 h (Figure 5c,d). Expression of *CACNA1S,* therefore, stimulated migration, presumably due to enhanced calcium influx into the cells. When the experiment was repeated with the mutant construct, no such enhanced

migration was evident, the cells showing identical kinetics to the non-transfected cells or control transfected cells (Figure 5c,d). The CHO cells expressing the mutant *CACNA1S*, therefore, were not capable of the enhanced migratory potential of the cells expressing WT *CACNA1S*.

3.5 | Overexpression of WT but not mutant CACNA1S impacts the cytoskeleton

Increases in filamentous actin (phalloidin staining) have been shown to be a prerequisite for cell migration and scratch closure (Xu et al., 2020). We therefore tested whether overexpression of WT *CACNA1S*, but not mutant *CACNA1S,* might cause an increase in phalloidin staining in CHO cells. Using FLAG Ab, to detect CACNA1S, and Phalloidin-TRTC, to stain for filamentous actin in our CHO stable lines, we demonstrated that FLAG Ab staining is present in both WT and mutant *CACNA1S* lines as expected. However, increased phalloidin staining was only observed after overexpression of the WT but not the mutant *CACNA1S* (Figure 6a). These results were quantified using imageJ (Figure 6b). The increase in phalloidin after overexpression of the WT protein was accompanied by a downregulation of vinculin and talin, two proteins involved in focal adhesions, while no similar loss was observed after overexpression of the mutant protein (Figure 6c).

4 | DISCUSSION

The striking features observed in our patients consist of molars with multiple supernumerary cusps, single rooted molars, and premolars with a single prominent cusp. Overall, the malformations appear to be the results of disorganization of both cusp and root patterning, with no obvious effect on mineralization of the dental hard tissues. All affected patients had the heterozygous c.865A>G; p.Ile289Val mutation in *CACNA1S* while unaffected family members did not have it. The same *CACNA1S* mutation has been reported in unrelated Thai patients with similar dental malformations. It is interesting to note that this mutation has been reported only in Thai patients. This restriction is most likely the result of a founder effect, as previously suggested (Laugel-Haushalter et al., 2018).

The expression of Cacna1s was identified in the tooth epithelium from early bud stages (E12.5) to postnatal (P5). No expression was observed at earlier stages of tooth development (E11.5), when the tooth placodes are initiated, suggesting that this calcium channel is involved in morphogenesis rather than induction and budding.

E14.5 is a key stage for tooth morphogenesis in mice with the formation of the primary enamel knot and the bending of the dental epithelium to create the cusps (Yamada et al., 2019). Interestingly, Cacna1s was expressed in the epithelial cells around the enamel knot but not in the knot itself, suggesting an interesting relationship with this group of non-dividing cells. Changes in calcium influx may, therefore, cause the initiation of more enamel knot areas in the molars, potentially triggering the extra cusps observed in patient molars. The morphology of the early tooth germ has been shown to be driven by differential proliferation and dynamic movement of epithelial cells (Yamada et al., 2019). Interestingly, overexpression of *CACNA1S* in CHO cells led to an increased migratory behavior and upregulation of phalloidin, linking changes in calcium influx to changes in cell behavior. Importantly, the mutant *CACNA1S* was unable to elicit such responses. The mutation in

patients might, therefore, lead to a reduced capacity of the dental epithelial cells to migrate. In our patients, molars became more complex, but the premolars became less complex as the result of the mutation. The differences in dental complexity may be due to the differences in tissue sensitivity to the mutation. As mice do not have premolars differences in expression between molars and premolars cannot be assessed.

Patients also showed root defects, with taurodontic teeth. Our study showed the expression of Cacna1s in HERS at postnatal day 5, suggestive of its role at the early stage of root morphogenesis. The mutation might disrupt the migration of the epithelial HERS, and, therefore, the invagination of the epithelial diaphragm, resulting in single-rooted molars in our patients, similar to that observed in ectodermal dysplasia models (Fons Romero et al., 2017).

The different subunits of the DHP channel appear to be expressed differentially during murine development, with *CACNA1G* expressed in the mesenchyme around the forming teeth, while *CACNA1A* and *B* were not expressed in the teeth during morphogenesis at E13.5 or E15.5 (Allen Brain atlas, https://developingmouse.brain-map.org/). These different patterns of expression can explain the different phenotypes associated with mutations in these different components (Duan, 2014). Muscular Dysgenesis (mdg) mice have a single nucleotide deletion in the α1 subunit (Knudson et al., 1989). These mice die at birth and their muscle and jaw phenotypes have been studied in detail (Chaudhari, 1992; Herring & Lakars, 1982). Whether these mice have a dental phenotype, however, has not been reported. The mdg mice, therefore, provide an interesting avenue for studying potential dental defects in more detail, and for assessing potential mechanisms that link calcium to additional cusps.

In conclusion, we demonstrate that defects in calcium signaling, due to a mutation in *CACNA1S,* lead to a variety of defects in dental development. Dental malformations can, therefore, be part of a calcium channelopathy. The mutation is likely to disrupt calcium flux, interfere with calcium homeostasis and subsequent calcium signaling in the cell, which is predicted to have a knock-on effect on cell dynamics and disrupt the normal induction/distribution of enamel knots. Since the clinical features of the malformation caused by the *CACNA1S* mutation described here resemble dens evaginatus but with larger cusps, we would like to coin the term “dens evaginatus giganticus” for this *CACNA1S* mutation-associated dental malformation.

Supplementary Material

Refer to Web version on PubMed Central for supplementary material.

ACKNOWLEDGMENTS

We thank our patients and their families for their kind cooperation and for allowing us to use their medical and dental information for the benefit of others. This work was supported by the Genomics Thailand Research Grant of Health Systems Research Institute (HSRI).

DATA AVAILABILITY STATEMENT

Datasets used and/or analyzed during the current study are available from the corresponding authors on reasonable request.

REFERENCES

Ahn Y, Sanderson BW, Klein OD, & Krumlauf R (2010). Inhibition of Wnt signaling by wise (Sostdc1) and negative feedback from Shh controls tooth number and patterning. Development, 137(19), 3221–3231. 10.1242/dev.054668 [PubMed: 20724449]

Chaudhari N (1992). A single nucleotide deletion in the skeletal muscle-specific calcium channel transcript of muscular dysgenesis (mdg) mice. The Journal of Biological Chemistry, 267(36), 25636–25639. [PubMed: 1281468]

Cho SW, Kwak S, Woolley TE, Lee MJ, Kim EJ, Baker RE, Kim HJ, Shin JS, Tickle C, Maini PK, & Jung HS (2011). Interactions between Shh, Sostdc1 and Wnt signaling and a new feedback loop for spatial patterning of the teeth. Development, 138(9), 1807–1816. 10.1242/dev.056051 [PubMed: 21447550]

Dong C, Wei P, Jian X, Gibbs R, Boerwinkle E, Wang K, & Liu X (2015). Comparison and integration of deleteriousness prediction methods for nonsynonymous SNVs in whole exome sequencing studies. Human Molecular Genetics, 24(8), 2125–2137. [PubMed: 25552646]

Duan X (2014). Ion channels, channelopathies, and tooth formation. Journal of Dental Research, 93(2), 117–125. 10.1177/0022034513507066 [PubMed: 24076519]

Eberl DF, Ren D, Feng G, Lorenz LJ, Van Vactor D, & Hall LM (1998). Genetic and developmental characterization of Dmca1D, a calcium channel alpha1 subunit gene in *Drosophila melanogaster*. Genetics, 148(3), 1159–1169. [PubMed: 9539432]

Fons Romero JM, Star H, Lav R, Watkins S, Harrison M, Hovorakova M, Headon D, & Tucker AS (2017). The impact of the Eda pathway on tooth root development. Journal of Dental Research, 96(11), 1290–1297. [PubMed: 28813629]

Gao S, Moreno M, Eliason S, Cao H, Li X, Yu W, Bidlack FB, Margolis HC, Baldini A, & Amendt BA (2015). TBX1 protein interactions and microRNA-96–5p regulation controls cell proliferation during craniofacial and dental development: Implications for 22q11.2 deletion syndrome. Human Molecular Genetics, 24(8), 2330–2348. 10.1093/hmg/ddu750 [PubMed: 25556186]

Geller F, Feenstra B, Zhang H, Shaffer JR, Hansen T, Esserlind AL, Boyd HA, Nohr EA, Timpson NJ, Fatemifar G, Paternoster L, Evans DM, Weyant RJ, Levy SM, Lathrop M, Smith GD, Murray JC, Olesen J, Werge T, … Melbye M (2011). Genome wide association study identifies four loci associated with eruption of permanent teeth. PLoS Genetics, 7(9), e1002275. 10.1371/journal.pgen.1002275 [PubMed: 21931568]

Harjunmaa E, Kallonen A, Voutilainen M, Hämäläinen K, Mikkola ML, & Jernvall J (2012). On the difficulty of increasing dental complexity. Nature, 483(7389), 324–327. [PubMed: 22398444]

Herring SW, & Lakars TC (1982). Craniofacial development in the absence of muscle contraction. Journal of Craniofacial Genetics and Developmental Biology, 1(4), 341–357. [PubMed: 7119092]

Jernvall J, & Thesleff I (2012). Tooth shape formation and tooth renewal: Evolving with the same signals. Development, 139(19), 3487–3497. [PubMed: 22949612]

Jonsson L, Magnusson TE, Thordarson A, Jonsson T, Geller F, Feenstra B, Melbye M, Nohr EA, Vucic S, Dhamo B, Rivadeneira F, Ongkosuwito EM, Wolvius EB, Leslie EJ, Marazita ML, Howe BJ, Moreno Uribe LM, Alonso I, Santos M, … Stefansson K (2018). Rare and common variants conferring risk of tooth agenesis. Journal of Dental Research, 97(5), 515–522. 10.1177/0022034517750109 [PubMed: 29364747]

Kangas AT, Evan AR, Thesleff I, & Jernvall J (2004). Nonindependence of mammalian dental characters. Nature, 432(7014), 211–214. [PubMed: 15538367]

Knudson CM, Chaudhari N, Sharp AH, Powell JA, Beam KG, & Campbell KP (1989). Specific absence of the alpha 1 subunit of the dihydropyridine receptor in mice with muscular dysgenesis. The Journal of Biological Chemistry, 264(3), 1345–1348. [PubMed: 2536362]

Laugel-Haushalter V, Morkmued S, Stoetzel C, Geoffroy V, Muller J, Boland A, Deleuze JF, Chennen K, Pitiphat W, Dollfus H, Niederreither K, Bloch-Zupan A, & Pungchanchaikul P (2018). Genetic evidence supporting the role of the calcium channel, CACNA1S, in tooth cusp and root patterning. Frontiers in Physiology, 9, 1329. 10.3389/fphys.2018.01329 [PubMed: 30319441]

Li C, Zhi D, Wang K, & Liu X (2022). MetaRNN: Differentiating rare pathogenic and rare benign missense SNVs and InDels using deep learning. Genome Medicine, 14(1), 115. 10.1186/s13073-022-01120-z [PubMed: 36209109]

Li X, Venugopalan SR, Cao H, Pinho FO, Paine ML, Snead ML, Semina EV, & Amendt BA (2014). A model for the molecular underpinnings of tooth defects in Axenfeld-Rieger syndrome. Human Molecular Genetics, 23(1), 194–208. 10.1093/hmg/ddt411 [PubMed: 23975681]

Liu H, Busch T, Eliason S, Anand D, Bullard S, Gowans LJJ, Nidey N, Petrin A, Augustine-Akpan EA, Saadi I, Dunnwald M, Lachke SA, Zhu Y, Adeyemo A, Amendt B, Roscioli T, Cornell R, Murray J, & Butali A (2017). Exome sequencing provides additional evidence for the involvement of ARHGAP29 in Mendelian orofacial clefting and extends the phenotypic spectrum to isolated cleft palate. Birth Defects Research, 109(1), 27–37. 10.1002/bdra.23596 [PubMed: 28029220]

Magnusson M (2018). GENMOD: Tool for annotating patterns of genetic inheritance in Variant Call Format (VCF) files. https://github.com/moonso/genmod.

Martinez-Ortiz W, & Cardozo TJ (2018). An improved method for modeling voltage-gated ion channels at atomic accuracy applied to human Ca_V channels. Cell Reports, 23(5), 1399–1408. 10.1016/j.celrep.2018.04.024 [PubMed: 29719253]

McKenna A, Hanna M, Banks E, Sivachenko A, Cibulskis K, Kernytsky A, Garimella K, Altshuler D, Gabriel S, Daly M, & DePristo MA (2010). The Genome Analysis Toolkit: A MapReduce framework for analyzing next-generation DNA sequencing data. Genome Research, 20(9), 1297–1303. 10.1101/gr.107524.110 [PubMed: 20644199]

Piétri-Rouxel F, Gentil C, Vassilopoulos S, Baas D, Mouisel E, Ferry A, Vignaud A, Hourdé C, Marty I, Schaeffer L, Voit T, & Garcia L (2010). DHPR alpha1S subunit controls skeletal muscle mass and morphogenesis. The EMBO Journal, 29(3), 643–654. 10.1038/emboj.2009.366 [PubMed: 20033060]

Schartner V, Romero NB, Donkervoort S, Treves S, Munot P, Pierson TM, Dabaj I, Malfatti E, Zaharieva IT, Zorzato F, Abath Neto O, Brochier G, Lornage X, Eymard B, Taratuto AL, Böhm J, Gonorazky H, Ramos-Platt L, Feng L, … Laporte J (2017). Dihydropyridine receptor (DHPR, CACNA1S) congenital myopathy. Acta Neuropathologica, 133(4), 517–533. 10.1007/s00401-016-1656-8 [PubMed: 28012042]

Seux D, Joffre A, Fosset M, & Magloire H (1994). Immunohistochemical localization of L-type calcium channels in the developing first molar of the rat during odontoblast differentiation. Archives of Oral Biology, 39(2), 167–170. 10.1016/0003-9969(94)90113-9 [PubMed: 8185503]

Splawski I, Timothy KW, Sharpe LM, Decher N, Kumar P, Bloise R, Napolitano C, Schwartz PJ, Joseph RM, Condouris K, Tager-Flusberg H, Priori SG, Sanguinetti MC, & Keating MT (2004). Ca(V)1.2 calcium channel dysfunction causes a multisystem disorder including arrhythmia and autism. Cell, 119(1), 19–31. 10.1016/j.cell.2004.09.011 [PubMed: 15454078]

Tsai FC, Kuo GH, Chang SW, & Tsai PJ (2015). Ca2+ signaling in cytoskeletal reorganization, cell migration, and cancer metastasis. BioMed Research International, 2015, 409245. 10.1155/2015/409245 [PubMed: 25977921]

Tucker AS, Headon DJ, Courtney JM, Overbeek P, & Sharpe PT (2004). The activation level of the TNF family receptor, Edar, determines cusp number and tooth number during tooth development. Developmental Biology, 268(1), 185–194. [PubMed: 15031115]

Waterhouse A, Bertoni M, Bienert S, Studer G, Tauriello G, Gumienny R, Heer FT, de Beer TAP, Rempfer C, Bordoli L, Lepore R, & Schwede T (2018). SWISS MODEL: Homology modelling of protein structures and complexes. Nucleic Acids Research, 46(W1), W296–W303. 10.1093/nar/gky427 [PubMed: 29788355]

Wu J, Yan Z, Li Z, Qian X, Lu S, Dong M, Zhou Q, & Yan N (2016). Structure of the voltage-gated calcium channel Ca(v)1.1 at 3.6 Å resolution. Nature, 537(7619), 191–196. 10.1038/nature19321 [PubMed: 27580036]

Xu J, Zhang Y, You S, Guo Y, Chen S, Chang Y, Zhang N, & Sun Y (2020). Paired box 9 regulates VSMC phenotypic transformation, proliferation and migration via sonic hedgehog. Life Sciences, 257, 118053. 10.1016/j.lfs.2020.118053 [PubMed: 32634424]

Yamada S, Lav R, Li J, Tucker AS, & Green JBA (2019). Molar bud-to-cap transition is proliferation independent. Journal of Dental Research, 98(11), 1253–1261. [PubMed: 31393749]

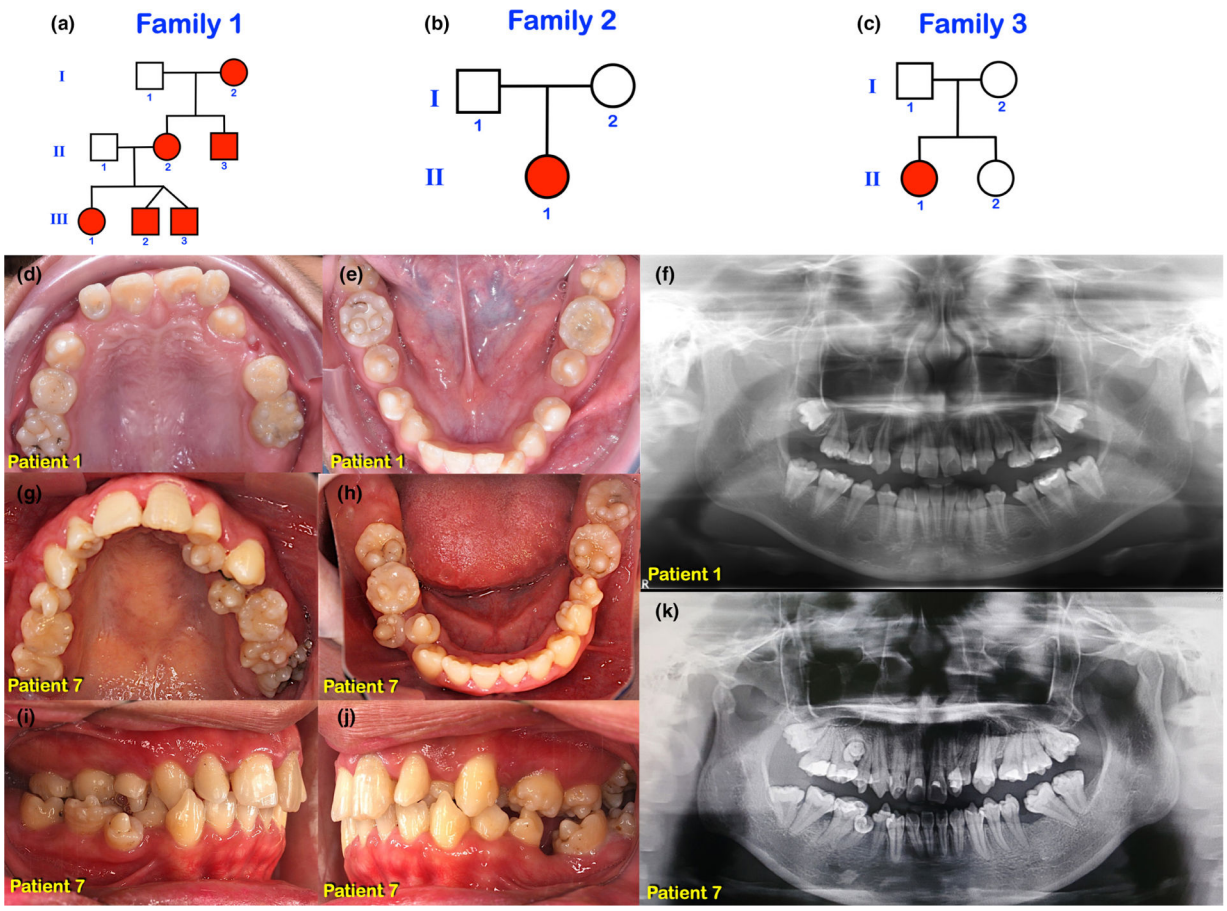

FIGURE 1.

Multiple supernumerary cusps and root defects in three Thai families. Pedigrees of (a) Family 1 and (b) Family 2. (c) Family 3. (d, e) Dental phenotypes in mixed dentition of patient III-1 of Family 1 (patient 1) at age 11 years. Multiple supernumerary cusps in molars. Single prominent cusp in premolars. (f) Patient 1. Panoramic radiograph taken at age 11 years. Note prominent supernumerary cusps in molars and premolars. Single-rooted molars are observed. Agenesis of the maxillary right first and second premolar and the maxillary left second premolar. (g–k) Patient 7 age 25 years. (g–j) Teeth are in permanent dentition. Molars have multiple supernumerary cusps. Premolars have single prominent cusps. (k) Panoramic radiograph showing prominent supernumerary cusps in molars and premolars. Single-rooted molars are observed.

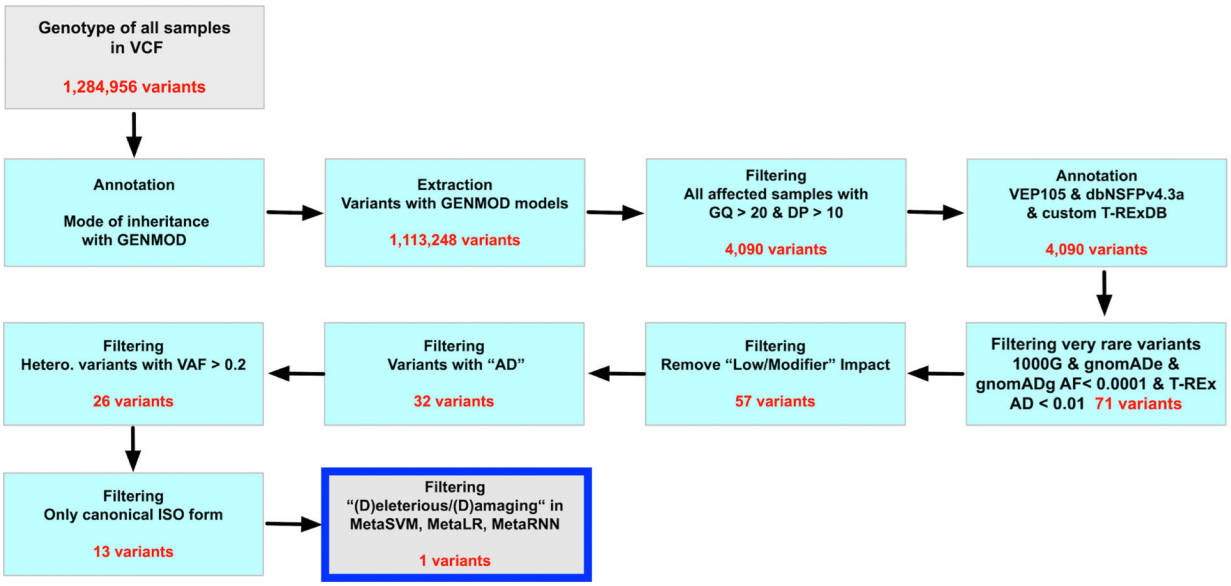

FIGURE 2.
The prioritization workflow to identify the etiologic mutation from WES data.

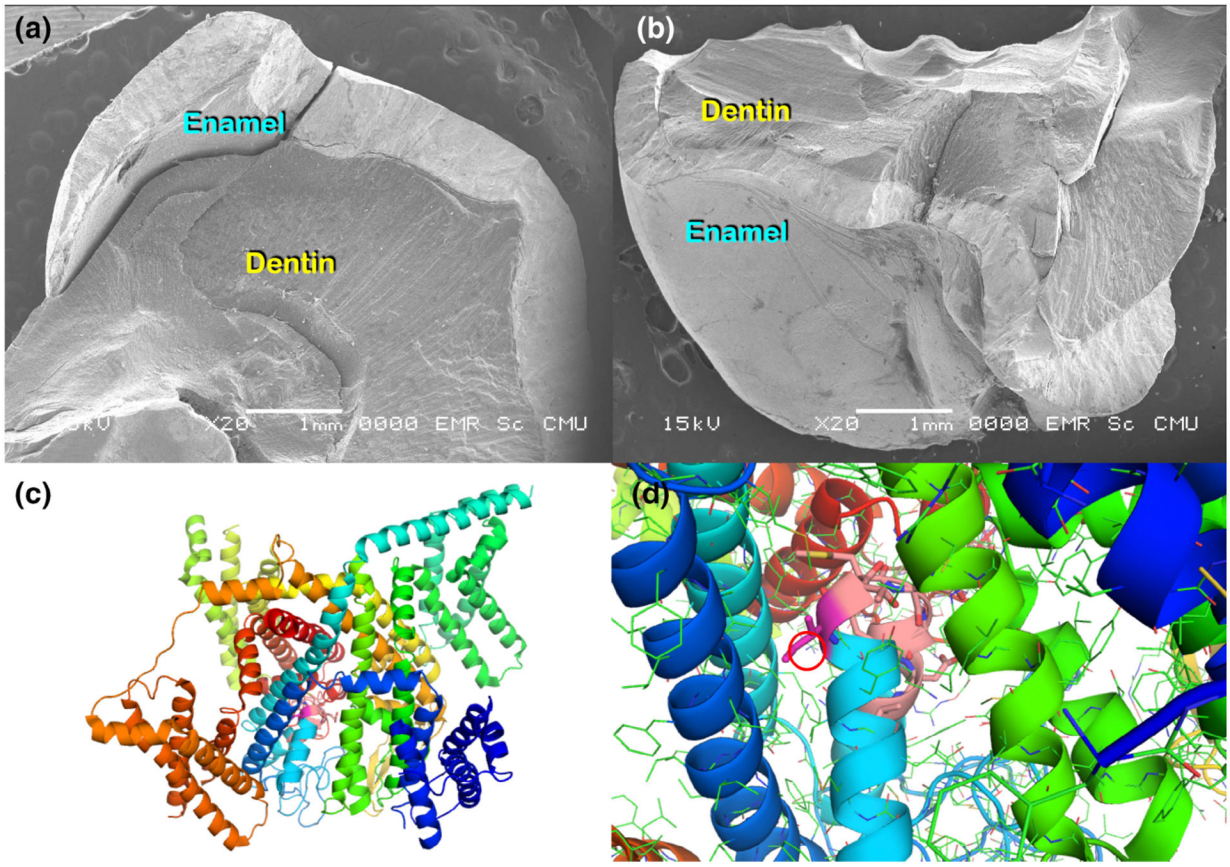

FIGURE 3.

Ultrastructure of a tooth and mutant protein modelling. (a, b) Scanning electron micrographs of an exfoliated deciduous molar. Note normal enamel and dentin layers. (c, d) Mutant protein modelling showing position of the mutation in the Ca_v 1 α-subunit structure. (c) The overall structure of the alpha subunit of $Ca_v1.1$ (Martinez-Ortiz & Cardozo, 2018; Wu et al., 2016). The I289 residue is shown in violet and the adjoining “selectivity filter” region is shown in salmon. (d) Close-up of the end of the 6th membrane helix (cyan) with the I289 residue and selectivity filter. The methyl group deleted in the I289V mutation is circled in red. The selectivity filter (pink) contains the ends of two short transmembrane helices and the short loop in-between, with the identical sequence: TMEGWTDV, in both proteins.

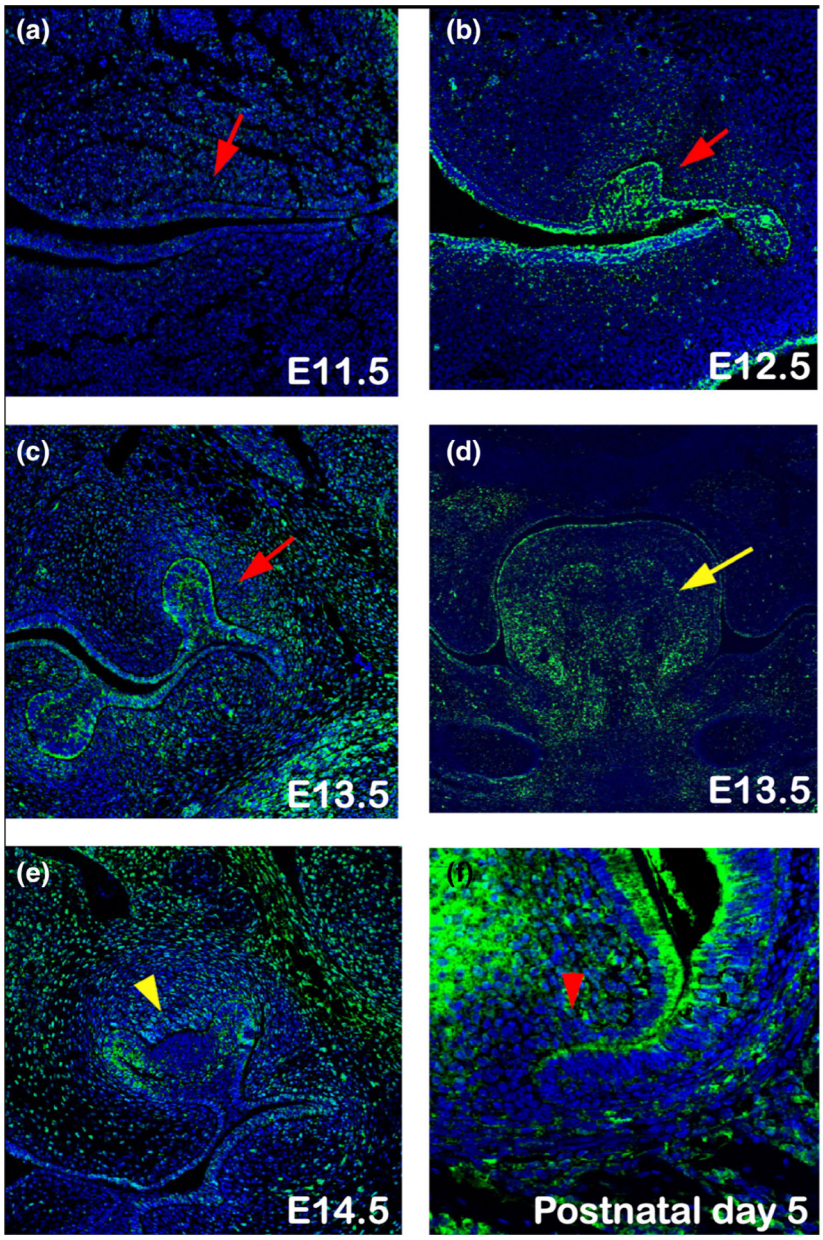

FIGURE 4.

Cacna1s expression during tooth development in mice. Frontal sections show Cacna1s expression in wild-type mice at Embryonic day (E) (a) 11.5, (b) E12.5, (c, d) E13.5, (e) E14.5, and (f) Postnatal day 5. Red arrows in figure (a–c) indicate tooth germs. Yellow arrow in (d) indicates the developing tongue. Yellow arrowhead in figure (e) indicates the enamel knot. Red arrowhead in figure (f) indicates the epithelial HERS. (a) No significant expression in the developing tooth is detected at E11.5. (b–d) Cacna1s is expressed in the developing dental epithelium at E12.5 and E13.5 in both upper and lower tooth germs, with high levels in the forming musculature of the lower jaw and tongue. (e) At E14.5, Cacna1s expression is observed in the dental epithelium, but not in the enamel knot. (f) In addition, Cacna1s expression is observed in the HERS at postnatal day 5 (f).

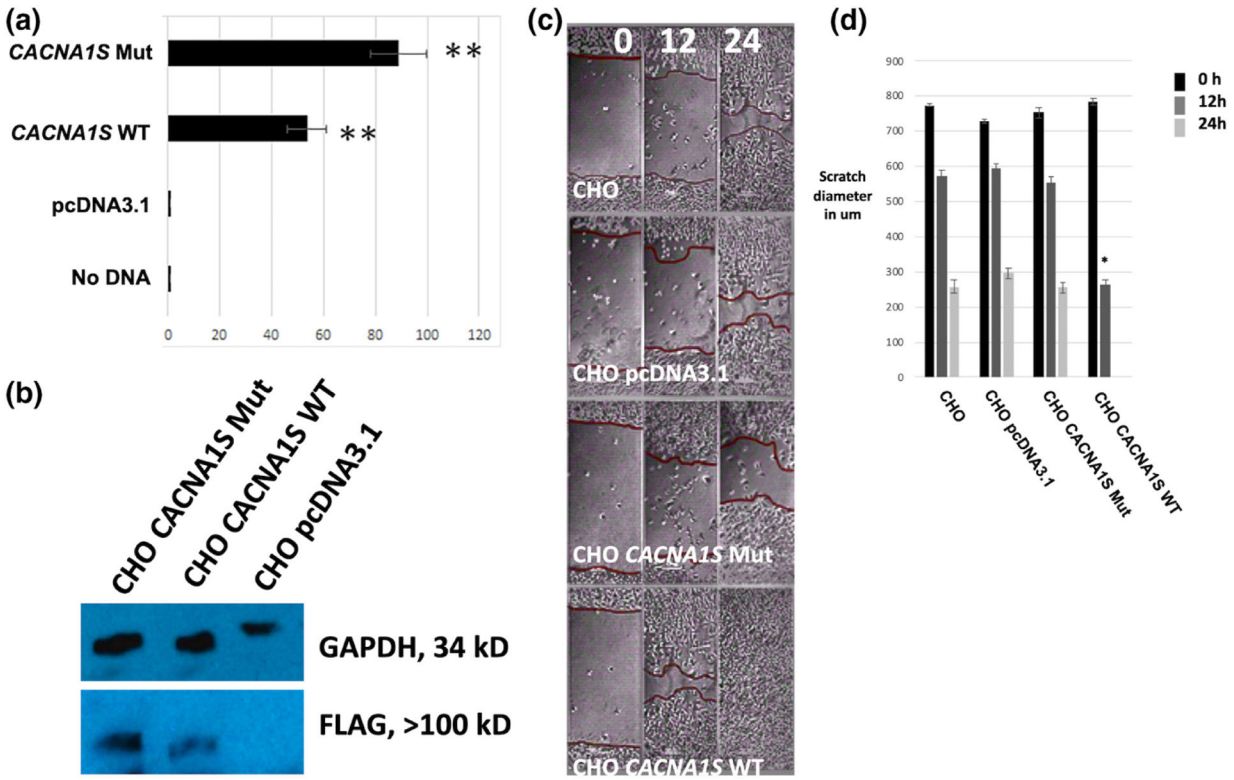

FIGURE 5.

Analysis of mutant and WT *CACNA1S* functions. (a) qPCR for *CACNA1S* expression in CHO cells stable lines. (b) Western blot showing GAPDH loading control (34 kDa) and recombinant CACNA1S using FLAG AB (>100 kDa). Robust antibody binding is evident in the WT and Mut OE lanes with no reactivity in the control lane, confirming the constructs are expressed. (c) Scratch/migration assay. Representative photos at T0, 12 h, and 24 h shown. (d) ImageJ analysis of the diameter of the open scratch in mm at 0, 12, and 24 h after the scratch was made ($n = 5$). *$p > 0.05$ **$p > 0.01$.

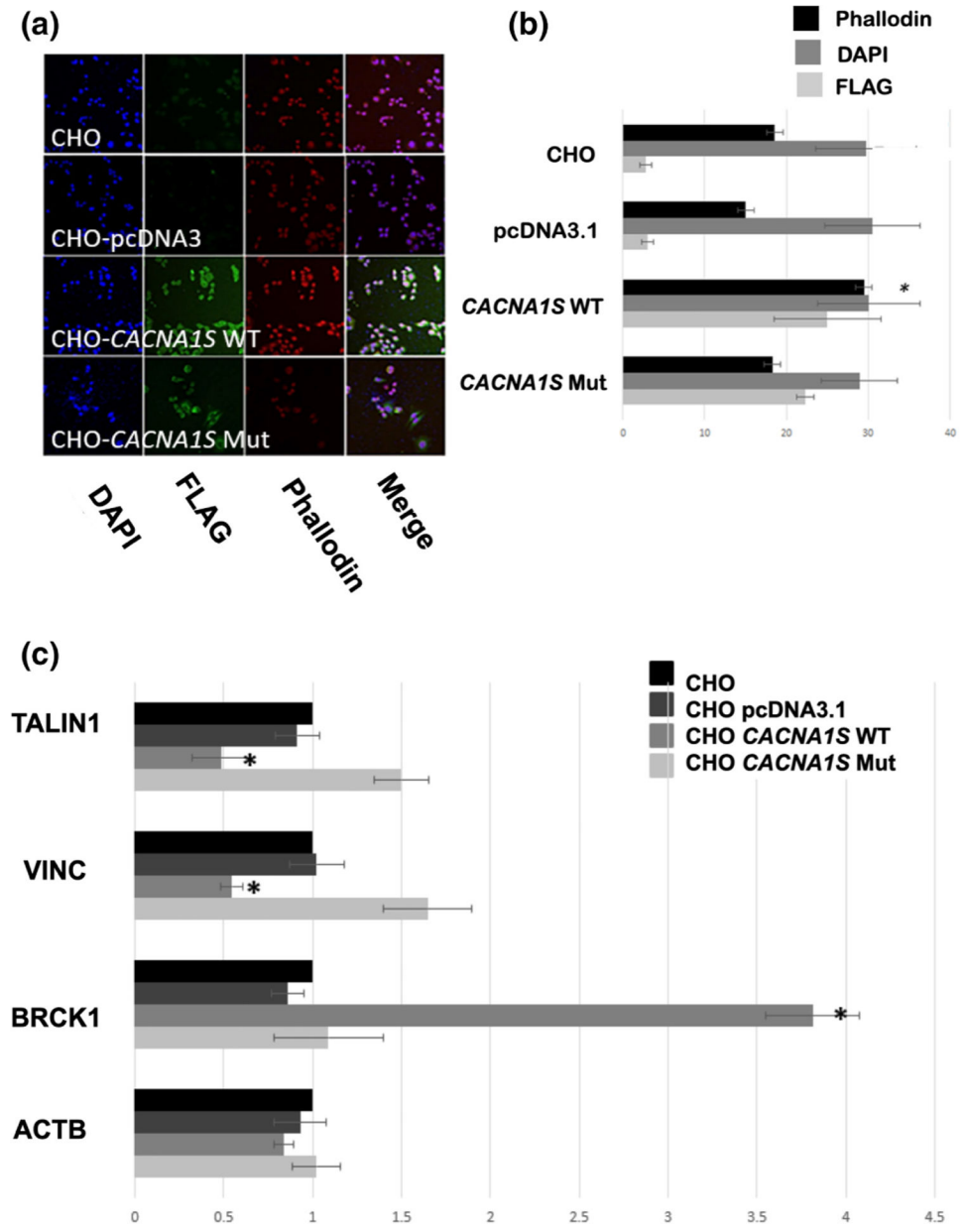

FIGURE 6.

Cytoskeletal changes after overexpression of mutant and WT CACNA1S. (a) Cells grown on coverslips were fixed and stained with DAPI (blue), FLAG/CACNA1S (green), and Phalloidin-TRTC (red). Image shown is a representative of many experiments. (b) Quantitation using ImageJ of phalloidin staining, three images for each cell and each color ($n = 3$) *$p > 0.05$. (c) qPCR was performed on CHO cells expressing control, CACNA1S WT or CACNA1S Mut to look at molecules shown to be involved in migration (Talin, Vinculin, Brck1 and Actb). Each bar is expressed as fold using $\Delta\Delta C_T$ of the listed genes versus Beta tubulin and represents the results of three independent RNA isolation/cDNA reactions. $N = 3$, *p value => 0.05.